

A METHOD OF PREDICTION OF THE PHASE CHANGE FRONT

Heon-Oh Choi*, Moon-Hyun Chun** and Yeon-Sik Kim***

(Received March 13, 1987)

Solidification on the outside wall of a convectively cooled tube is investigated. Experiments on solidification of an initially stagnant liquid onto a convectively cooled vertical tube situated concentrically within the containment vessel are carried out. The transient temperatures of the tube at various axial locations are obtained as a function of time. Using these data for the wall temperatures, the transient position of the phase change front is predicted by the optimization technique proposed in Choi, H.O. and Chun, M.H. (1985). Transient shapes of the solid-liquid interface are photographically recorded at pre-selected times in order to compare with the predictions of the optimization technique. The natural convection flow due to the temperature variations developed in the liquid phase has shown a drastic influence on the freezing process and the shape of the frozen-layer.

Key Words : Phase Change, Liquid-Solid Interface, Finite Element Method, Optimization Technique, Fibonacci Search.

NOMENCLATURE

g_m, g_n	: Shape function
h	: Heat transfer coefficient for coolant flow
k	: Thermal conductivity of the solid phase
k_t	: Thermal conductivity of the tube
$q_c'(t)$: Rate of heat flow per unit length of the tube by convection
q_l''	: Heat flux of the liquid phase at the liquid-solid interface
q_s''	: Heat flux of the solid phase at the liquid-solid interface
r_i	: Inner radius of the tube
r_o	: Outer radius of the tube
$r_s(t)$: Transient position of the liquid-solid interface
t	: Time
$T(r,t)$: Temperature of the solid phase
$T_b(t)$: Bulk temperature of the coolant
T_f	: Fusion temperature
T_o	: Initial temperature of liquid and surface temperature of containment vessel
$T_w(r_i,t)$: Temperature of the inside tube wall
$T_w(r_o,t)$: Temperature of the outside tube wall
ΔT_i	: Inner temperature difference, $T_i - T_b$
ΔT_o	: Initial liquid superheat, $T_o - T_f$
U	: Overall heat transfer coefficient

Greek Symbols

α	: Thermal diffusivity of the solid phase
ρ	: Density of the solid phase
λ	: Latent heat of fusion

Superscripts

k	: Time step
Δ	: Quantities expressed by the finite element approximation
*	: Shape function along the boundary

Subscripts

ℓ	: Liquid phase
s	: Solid phase
m, n	: Node indices

1. INTRODUCTION

The phenomena of liquid-solid phase change are of practical interest in a wide range of technical applications. For example, the melting and solidification processes have been extensively studied for the latent heat-of-fusion energy storage design (Sparrow, et al, 1979, Sparrow, et al, 1981, Ho, et al, 1984), the assessment of molten fuel relocation following hypothetical core-disruptive accidents in liquid-metal-fast-breeder reactors (Epstein, et al, 1980, Chun, et al, 1976, Chun, et al, 1985), casting of metals (Siegel, 1982), and desalination of water. The major characteristics of the melting and freezing problems include the movement of a phase boundary induced by the diffusion of energy or mass, and the nonlinearity associated with the moving phase boundary extremely complicates its analysis.

Those works reviewed by the authors could be classified into a few broad categories: (1) the exact closed form solutions (Stefan, 1981, Carslaw, et al, 1959) which exist for some special cases where conduction is the sole mode of heat transfer, (2) approximate analytical and numerical solutions (Chun, et al, 1985, Siegel, 1982, Stefan, 1981, Carslaw, et al, 1959, Sparrow, et al, 1977) which take into consideration the effects of natural and/or forced convection, and (3) other parametric or ad hoc solutions (Gupta, et al, 1985, Shamsundar, et al, 1979) that have been proposed for special applications.

The main objective of the present work is to examine the usefulness of the proposed method of the phase-change-front prediction based on the optimization technique (Choi, et al, 1985) by application to a special case. This paper describes a combined experimental and theoretical study of the phase change front when solidification of an initially stagnant superheated molten fluid occurs on the outside wall of a convectively cooled vertical tube. When the wall temperature of the cooled tube falls below the solidification temperature of the phase change material (molten paraffin wax was used in the present work) freezing occurs along the outside wall of the cooled tube. During solidification, the phase change front moves into the liquid and the shape of the freezing interface responds to the rate at which heat is being locally removed. The thickness of the frozen layer will grow until the amount of the local heat conducted through the frozen layer from the solidification interface to the convectively cooled tube wall becomes equal to the amount of the local heat added to the

* Department of Thermal Engineering, Korea Institute of Machinery & Metals, Changwon 615, Korea

** Department of Nuclear Engineering, Korea Advanced Institute of Science & Technology, Seoul 131, Korea

*** Korea Advanced Energy Research Institute, Daejeon 300, Korea

interface by the superheated liquid surrounding the liquid-solid interface. A steady-state condition will be achieved if the net amount of energy being locally removed becomes zero at all locations along the liquid-solid interface.

To predict the transient position of the liquid-solid interface by the suggested method(Choi, et al, 1985), one needs the temperature of the wall on which phase change is taking place. This technique is suitable to obtain information about the moving liquid-solid interface of the nontransparent phase change material, in particular, where the photographic method can not be used. It is also useful for the case of inward solidification of flowing fluid in a tube, where direct measurement of the liquid-solid interface is not possible, whereas the tube wall temperature measurement is relatively easy.

2. EXPERIMENTAL APPARATUS AND PROCEDURE

2.1 Test Apparatus

To examine the applicability of the minimization technique developed to predict the phase change front(Choi, et al, 1985), one needs two sets of experimental data taken simultaneously. The first data are the experimental values of solid-liquid interface position as a function of time, and the other is the wall temperature of the tube on which solidification is taking place. The former is needed to compare directly with predictions of theory, while the latter is used as a boundary condition in the minimization formulation for the prediction of the phase-change front.

The experimental apparatus designed to obtain the above two sets of data was similar to the one used by Sparrow et al., (1979).

A schematic diagram of the test cell is shown in Fig. 1. The major components of the test apparatus were: (1) a cooled cylindrical tube which was immersed in the liquid paraffin during a data run so that the freezing could take place on the outside surface of the tube wall; (2) a cylindrical containment vessel situated in a temperature controlled water bath to contain a liquid paraffin (n-octadecane); (3) a constant temperature water bath and auxiliary systems for controlling the temperature of the cooled-tube and temperature of the environment surrounding the phase-change medium.

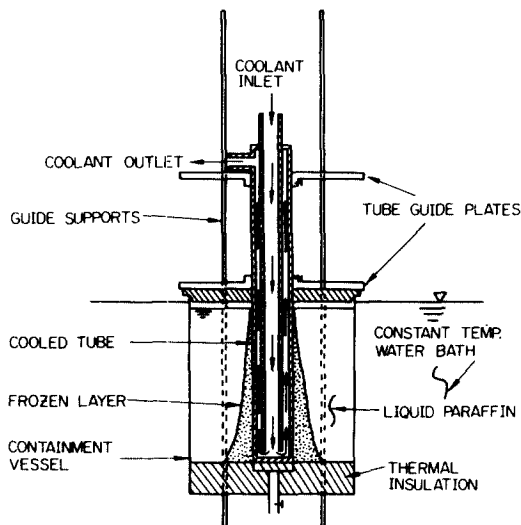


Fig. 1 Schematic diagram of test cell.

The cooled cylindrical tube, which is concentric with the containment vessel, is a tube within a tube. The outer tube, which is 2.54cm in diameter, is a thick-walled (0.2cm in thickness) copper pipe. The inner tube, on the other hand, is of thin-walled copper (0.6cm in diameter). As shown in Figs. 1 and 2, the coolant enters at the top of the inner tube and flows axially downward. At the bottom of the tube, the coolant reverses flow direction and passes upward through the annular space between the tubes, and finally flowing out at the top. Dimensions are shown in Table 1.

Table 1 Test section geometry

	Inner tube	Outer tube	Containment vessel
I.D. (mm)	4.0	21.0	150.0
O.D. (mm)	6.0	25.4	155.0
Length(mm)	270.0	300.0	195.0
Material	Copper	Copper	Stainless steel

The containment vessel, which is situated in a temperature controlled water bath, is 15cm in diameter and 20cm high. To isolate the lower regions of the frozen layer from thermal interactions with the lower wall of the containment vessel, a 5cm thick compact-styrofoam insulation layer was attached to the bottom of the vessel. In addition, the insulation was covered with plastic-coated contact paper to insure a smooth surface.

The constant temperature water bath was housed in an acryl tank whose dimensions were 50cm deep, and 80 × 60cm in horizontal cross section. Temperature control and its uniformity was achieved by a thermostatically activated heating device which also served to circulate the water through the bath. As can be seen in Figs. 1 and 2, the constant temperature water bath enables to maintain the surface temperature of the vessel at a constant value T_0 .

To measure the wall temperature of the cooled tube on which solidification takes place, eight thermocouples were installed on the inside surface of the outer tube, respectively at axial positions located 1.5, 3.0, 4.5, 6.0, 7.5, 9.0, 10.5, and 12.0cm from the lower end.

Controlled vertical positioning and axial movement of the cooled tube was performed by the support and guide structures shown at the top of Fig. 1. Four vertical supports, welded to the outer surface of the containment vessel,

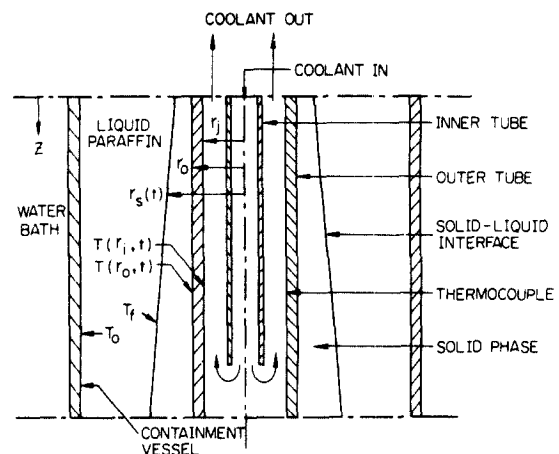


Fig. 2 Physical model for solidification on the outside wall of a convectively cooled tube.

positioned a pair of guide plates through which the cooled-tube is locked in place. Each guide plate is 0.4cm thick stainless-steel disk machined with a center hole whose diameter is slightly larger than that of the cooled-tube. Each disk is equipped with a set screw.

The instrumentation for the experiments included analog voltmeters, which could be read to $1\mu V$, for detecting the thermocouple outputs and associated recording equipment.

2.2 Test Parameters

There are three temperature parameters that play a decisive role in the solidification process (Sparrow, et al, 1979): (1) the temperature $T_w(r, t)$ of the cooled tube on which the freezing occurs, (2) the solid-liquid interface temperature T_f (i.e., temperature of the phase change front), and (3) the initial temperature T_o of the superheated liquid. Of these, the fusion temperature T_f is one of the physical properties of the phase change material. The physical properties of the 97 percent n-octadecane paraffin used in the present work are given in Table 2 (Hale, et al, 1971). The other two temperatures constitute, along with the duration time of a data run, the main controllable test parameters. In the actual test, the temperature of the cooled tube $T_w(r, t)$ was controlled by controlling the coolant temperature T_b and the coolant flow rate.

Table 2 Physical properties of N-octadecane

	Solid	Liquid
Melting point(°C)	28	—
Heat of fusion(J/kg)	243000	—
Density(kg/m ³)	814(at 27°C)	774(at 32°C)
Thermal conductivity (W/m ³ K)	0.15(at 28°C)	—
Specific heat(J/kg ³ K)	2160	—
Viscosity(kg/sec-m)	—	0.00268(at 40°C)

In the present experiments, two levels of coolant temperature (i.e., $T_b = 17$ and $3^\circ C$, respectively) and two levels of initial molten fluid temperatures (i.e., $T_o = 40$ and $34.5^\circ C$) were chosen as the main prescribable parameters. To specify test conditions, however, the above parameters will be reduced to a pair of temperature differences as following:

$$\Delta T_i = T_f - T_b, \quad \Delta T_o = T_o - T_f \quad (1a, b)$$

physically, ΔT_i is the temperature difference between the solidification temperature of the liquid paraffin and the coolant temperature, whereas ΔT_o is the initial superheat of the liquid paraffin. These quantities will, in subsequent discussion, be referred to respectively as the "inner temperature difference" and "liquid superheat".

2.3 Test Procedure

To obtain the experimental data of the phase change front position versus time and the transient wall temperature of the outer tube $T_w(r, t)$, a succession of data runs of different duration times was performed for fixed values of ΔT_i and ΔT_o .

The constant temperature water bath and the containment vessel were first charged with the water and the molten paraffin wax. Prior to each data run, thermal equilibria were separately established in the liquid paraffin and in the cooled tube at the desired values of T_o and T_w . During this preparatory period, the cooled tube was positioned above the paraffin containment vessel. The wall temperature of the containment vessel is maintained at a uniform and constant temper-

ature during each data run by the temperature controlled water bath.

The data run was initiated by lowering the cooled tube into the liquid paraffin and by circulating the coolant through the tube, and a frozen layer was formed on the outside wall of the tube immediately. Inside wall temperature of the outer tube was measured as a function of time while the data run was allowed to proceed for a preselected duration. After duration of preselected times (i.e., at 1, 2, 3, 5, 10, 15, 20, 30, 45, and 60 minutes for each data run), the cooled tube, along with the attached frozen paraffin layer, was instantly raised vertically upward and pulled out of the containment vessel. Photographs of each frozen layer specimen along with a reference scale were taken, and measurements of the frozen-layer thickness at various axial positions were made and recorded.

2. MINIMIZATION FORMULATION TO PREDICT PHASE CHANGE FRONT

3.1 Mathematical Formulation

When a phase change occurs, the shape of the solid-liquid interface becomes a curved surface in general. However, if the surface is sufficiently smooth, it is possible to represent the phase change process in one-dimensional form. Therefore, when solidification is taking place on the outside wall of a circular tube, while the inside wall of the tube is convectively cooled as shown in Fig. 2, the governing equation, initial and boundary conditions for the solid phase can be expressed as follows:

$$\frac{1}{\alpha} \frac{\partial T}{\partial t} - \frac{1}{r} \frac{\partial}{\partial r} \left(r \frac{\partial T}{\partial r} \right) = 0, \quad \text{in } r_s(t) > r > r_o, t > 0 \quad (2)$$

$$T(r, t) = T_f, \quad \text{at } r = r_s(t), t > 0 \quad (3)$$

$$r_o k \frac{\partial T}{\partial r} - r_i U (T - T_b) = 0, \quad \text{at } r = r_o, t > 0 \quad (4)$$

$$r_s(t) = r_o, \quad \text{at } t = 0 \quad (5)$$

Where $T(r, t)$ and $r_s(t)$ denote the temperature of the solid phase and the transient position of the solid-liquid interface, respectively.

Equation (3) expresses the fact that the temperature of the solid-liquid interface is at the fusion temperature T_f of the phase change material. Equation (4) is a mixed boundary condition at the convectively cooled wall, where U is the overall heat transfer coefficient defined by

$$U = \frac{1}{(1/h) + r_i [\ln(r_o/r_i)/k_t]} \quad (6)$$

In Eq. (6), a perfect thermal contact between the outside wall of the tube and the solidified-layer is assumed.

The initial condition, Eq. (5), denotes that no presolidified-layer exists at the onset of solidification.

The transient position of the solid-liquid interface is determined by

$$\rho \lambda \frac{\partial r_s(t)}{\partial t} = -(q_s'' - q_l''), \quad \text{at } r = r_s(t) \quad (7)$$

where ρ , λ , q_s'' and q_l'' are the density, the latent heat of fusion, the heat flux of the solid phase and the heat flux of the liquid phase at the solid-liquid interface, respectively.

$r_s(t)$ is still unknown when both q_l'' and q_s'' are unknown. Notice that the q_l'' is difficult to obtain when convection is present in the liquid phase. Therefore, in order to trace the transient solid-liquid interface $r_s(t)$ in the present work, another boundary condition, Eq. (8), is used. That is, when the thermal conductivity of the tube wall is sufficiently large, the

measured temperature of the inside wall of the tube, $T_w(r_i, t)$, is related to the outside wall temperature of the tube, $T_w(r_o, t)$, by the following equation :

$$T_w(r_o, t) = q'_c(t) \frac{\ln(r_o/r_i)}{2\pi k_t} + T_w(r_i, t) \quad (8)$$

where q'_c is the rate of heat flow per unit length of the tube by convection and it is given by

$$q'_c(t) = 2\pi r_i h [T_w(r_i, t) - T_b(t)] \quad (9)$$

Thus, Eq. (8) can be evaluated by experimentally measuring the inside wall temperature of the convectively cooled tube $T_w(r_i, t)$.

The outside wall temperature, $T_w(r_o, t)$, can also be approximated by the temperature of the solid phase at $r = r_o$, if perfect thermal contact between the outside wall of the tube and the solidified-layer is assumed. Thus,

$$T(r, t) = T_w(r_o, t) \quad \text{at } r = r_o \quad (10)$$

This additional boundary condition, Eq. (10), in addition to Eqs. (2)~(5), is employed to predict the transient position of the solid-liquid interface.

Since $r_s(t)$ is an unknown function, the above problem is difficult to solve in its original form. Therefore, the above problem is transformed into an equivalent minimization problem of finding the moving boundary $r_s(t)$ which minimizes the difference between the temperatures given by Eq. (10) and the temperature at $r = r_o$ calculated from the governing equation. Mathematically, the problem is to determine $r_s(t)$ which minimizes

$$\int_0^t |T_w(r_o, t) - T(r_o, t)|^2 dt \quad (11)$$

and satisfies

$$\frac{1}{\alpha} \frac{\partial T}{\partial t} - \frac{1}{r} \frac{\partial}{\partial r} \left(r \frac{\partial T}{\partial r} \right) = 0, \text{ in } r_s(t) > r > r_o, t > 0 \quad (12)$$

$$2\pi r_o k \frac{\partial T}{\partial r}(r_o, t) - q'_c(t) = 0, T[r_s(t), t] = T_f \quad (13a, b)$$

$$r_s(0) = r_o \quad (14)$$

It may be noted here that three major assumptions were made in the above mathematical formulation :

(1) Since the variation of the solidified-layer thickness as a function of time along the tube axis is sufficiently small compared to the radial growth rate in the present experiment, one dimensional approximation is made. Therefore, the governing equation for the solidified-layer at each measuring point is given by Eq. (2).

(2) Since the thermal resistance of the tube wall is extremely small compared to the thermal resistance of the solidified-layer of the phase change material used in the present experiments (i.e., paraffin wax), a steady-state heat conduction in the tube wall is assumed.

(3) The thermophysical properties of the frozen-layer as well as the tube were assumed to be constant.

3.2 Numerical Procedure

The proposed minimization problem is discretized using the finite element, suitable for numerical calculation. The solution domain of the state equation, Eq. (12), is continuously deforming with moving boundary $r_s(t)$, as shown in Fig. 3. Therefore, the space-time finite element is used to easily incorporate the continuously deforming domain. The isoparametric space-time finite element approximations for the temperature $T(r, t)$ and domain variables r and t can be written as

$$\hat{T}(r, t) = T_m G_m(\xi, \eta), \hat{r} = r_m g_m(\xi, \eta), \hat{t} = t_m g_m(\xi, \eta) \quad (15a, b, c)$$

Where T_m , r_m and t_m are nodal values, and the summation convention is represented by the dummy index m . A linear

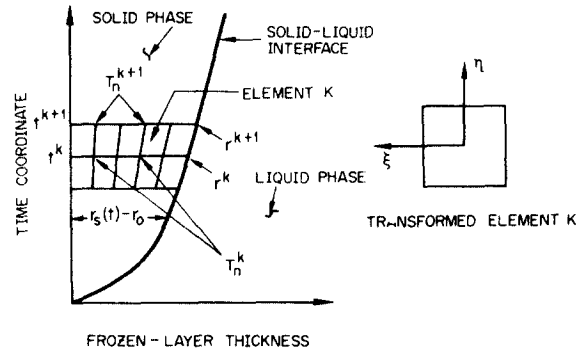


Fig. 3 Solution domain and transformed domain.

interpolation function is used as the shape function as shown in Fig. 3.

To have only one design variable in the discretized form and to increase the efficiency of calculation, one discretization in the time coordinate is made.

The Galerkin finite element procedure is applied to the state equation, Eq. (12), with one discretization in the time coordinate. Thus,

$$2\pi \int_{t^k}^{t^{k+1}} \int_{r_o}^{r_s(t)} g_m \left[\frac{1}{\alpha} \frac{\partial \hat{T}}{\partial t} - \frac{1}{r} \frac{\partial}{\partial r} \left(r \frac{\partial \hat{T}}{\partial r} \right) \right] r dr dt = 0 \quad (16)$$

Using the Green-Gauss theorem on the transient term as well as on the diffusion term and then applying the initial and boundary condition, Eq. (16) becomes

$$2\pi \int_{t^k}^{t^{k+1}} \int_{r_o}^{r_s(t)} \left(-\frac{1}{\alpha} \frac{\partial g_m}{\partial t} g_n + \frac{\partial g_m}{\partial r} \frac{\partial g_n}{\partial r} \right) r dr dt T_n + 2\pi \int_{r_o}^{r_s(t^{k+1})} \frac{1}{\alpha g_m^* g_n^*} r dr T_n - \int_{t^k}^{t^{k+1}} \frac{1}{k} g_m^* q'_c(t) dt = 0 \quad (17)$$

where g_m^* and g_n^* in the second term and g_m^* in the third term represent the shape function defined on the boundary of the solution domain, and $dr dt = |J| d\xi d\eta$ and J is the Jacobian defined by $\partial(r, t)/\partial(\xi, \eta)$.

The design variable $r_s(t)$ is reduced to $r_s(t^{k+1})$ (see Fig. 3) and the objective function, Eq. (11), is reduced to

$$|T_w(r_o, t^{k+1}) - T(r_o, t^{k+1})|^2 \quad (18)$$

Therefore, the discretized version of the minimization problem using the space-time finite element with one discretization in the time coordinate is reduced to a problem of finding $r_s(t^{k+1})$ which minimizes the objective function, Eq. (18), and satisfies the state equation Eq. (17).

In this approach, the results of the previous time step are used as the initial condition of the present step.

Since the number of the design variables is reduced to one in the formulation of the minimization problem in the numerical procedure, the Fibonacci search technique(Luenberger, 1973) is used to find $r_s(t^{k+1})$, simultaneously solving the state equation, Eq. (17).

4. EXPERIMENTAL RESULTS AND COMPARISON WITH MODEL

To test the applicability of the present model by comparing with experimental data and to examine the effects of the two temperature parameters (T_o and T_i) on the phase change front velocity, four data runs were made at two levels of the inner temperature difference and at two different liquid superheats : the first two data runs were made at two levels of initial liquid superheat (i.e., $\Delta T_o = 12$ and 6.5°C , respectively) while ΔT_i is maintained constant ($\Delta T_i = 9^\circ\text{C}$).

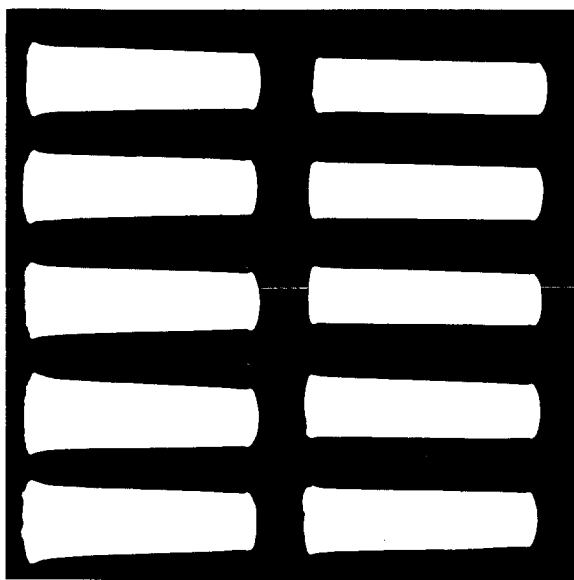


Fig. 4 Typical solidified-layer growth pattern in a superheated liquid ($\Delta T_i = 25^\circ\text{C}$, $\Delta T_o = 6.5^\circ\text{C}$); Run times (top left to bottom right): 1, 2, 3, 5, 10, 15, 20, 30, 45 and 60 min.

For the other two data runs, ΔT_i was raised and fixed at 25°C while using the two levels of initial liquid superheat (i. e., $\Delta T_o = 12$ and 6.5°C).

For each data run, ten different run times were used varying from one to sixty minutes, and photographs of each frozen layer specimen were taken to obtain a quantitative data on the timewise growth of the frozen-layer. A typical solidified-layer growth pattern in a superheated liquid is displayed photographically in Fig. 4. The test conditions for this case were $\Delta T_i = 25^\circ\text{C}$ and $\Delta T_o = 6.5^\circ\text{C}$, respectively.

The patterns of the frozen-layer yield a gently contoured surface, as shown in Fig. 4, with the thickness of the layer increasing from top to bottom in contrast to the near-perfect cylinder for the non-superheating case (Sparrow, et al, 1979).

In the case of the solidification of a superheated liquid, the radial temperature variation in the liquid, ranging from the fusion temperature T_f at the solid-liquid interface to the reservoir temperature T_o at the wall of the containment vessel, is developed as freezing proceeds.

As a results, due to the density variations associated with this radial variations of liquid temperature, a closed-loop natural convection flow would be induced: there will be a natural convective upflow along the highest temperature wall of the containment vessel and a downflow occurs along the solid-liquid interface at the lowest temperature. The upflow adjacent to the containment vessel extract heat from the reservoir tank and the heat is lost in the downflowing liquid adjacent to the solid-liquid interface. As a result, the temperature of the downward liquid is decreased and subsequently the heat flux transferred from the liquid phase to the interface decreases along the downward rapidly at the bottom of the tube and consequently the patterns of the solid-liquid interface, as shown in Fig. 4, are built up.

4.1 Effect of Cooling Rate

According to Eq. (9), an increase of ΔT_i by decreasing T_b in Eq. (1a) the cooling rate of the tube $q_c(t)$ will be increased. During the transient period, the necessary condition for solidification is $q_c'' > q_i'$ in Eq. (7). The rate of solidification is

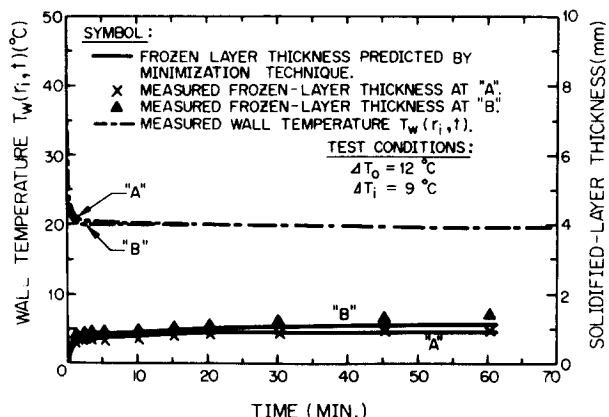


Fig. 5 Comparison between experimental results and minimization theory for solidified-layer thickness versus time at two axial positions on the tube (A=9 and B=3cm from the bottom).

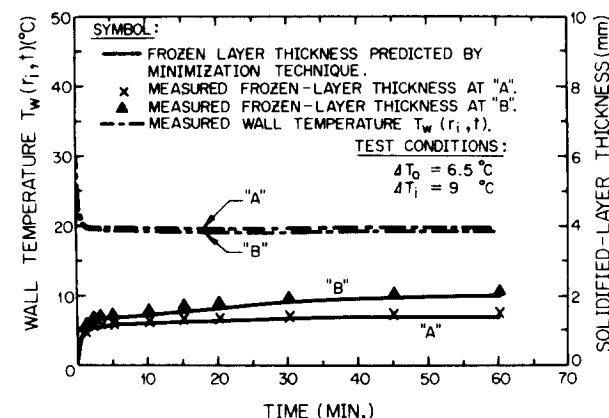


Fig. 6 Comparison between experimental results and minimization theory for solidified-layer thickness versus time at two axial positions on the tube (A=9 and B=3cm from the bottom).

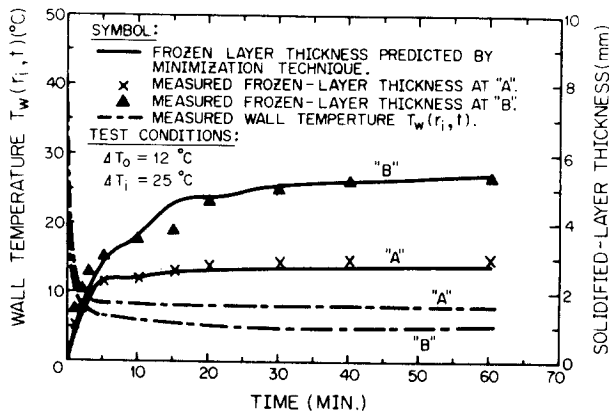


Fig. 7 Comparison between experimental results and minimization theory for solidified-layer thickness versus time at two axial positions on the tube (A=9 and B=3cm from the bottom).

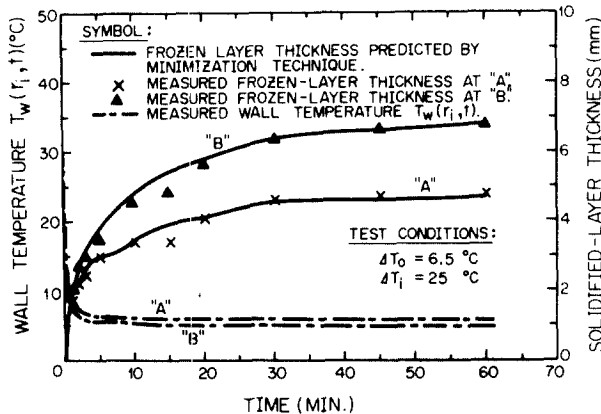


Fig. 8 Comparison between experimental results and minimization theory for solidified-layer thickness versus time at two axial positions on the tube (A=9 and B=3cm from the bottom).

determined by the quantity given by the right hand side of Eq. (7). Since an increase of $q_c^*(t)$ is equivalent to increasing q_s^* , the thickness of the frozen-layer increases when ΔT_1 is increased at a fixed ΔT_0 . This deduced result can be confirmed by comparing the two sets of experimental data shown in Fig. 5 ($\Delta T_1 = 9^\circ\text{C}$, $\Delta T_0 = 12^\circ\text{C}$) and Fig. 7 ($\Delta T_1 = 25^\circ\text{C}$, $\Delta T_0 = 12^\circ\text{C}$) or Fig. 6 ($\Delta T_1 = 9^\circ\text{C}$, $\Delta T_0 = 6.5^\circ\text{C}$) and Fig. 8 ($\Delta T_1 = 25^\circ\text{C}$, $\Delta T_0 = 6.5^\circ\text{C}$). For example, the final thickness of the frozen layer in Fig. 5 is 1.1mm(Curve B), whereas the final thickness in Fig. 7 is 5.4mm(Curve B) for the same duration time of 60 minutes.

4.2 Effect of Initial Molten Fluid Superheat

According to Eq. (1b), ΔT_0 can be varied by varying the initial temperature of the molten paraffin wax T_0 . For the solidification of the molten fluid, the latent heat as well as the sensible heat of the molten fluid must be removed. When ΔT_0 is decreased by decreasing the initial temperature of the molten fluid T_0 , the amount of sensible heat to be removed for solidification becomes smaller. Thus, a decrease in ΔT_0 at a fixed ΔT_1 will bring about an increase in the final thickness of the frozen layer and a shorter freezing time. Comparison of the solidified-layer thickness versus time curves shown in Figs. 5 and 6 as well as the curves shown in Figs. 7 and 8 confirms the above physical deductions. For example, the final thickness of the frozen layer in Fig. 7 is about 5.4mm(curve B) whereas the curve B of Fig. 8 is about 6.8mm for the same duration time of 60 minutes.

4.3 Comparison between Theory and Experimental Data

Figures 5 and 6 show that the wall temperature of the outer tube $T_w(r_i, t)$, while freezing continued on its outer surface, was remained at fairly constant value (about 20°C) substantially below the freezing temperature of the liquid paraffin ($T_f = 28^\circ\text{C}$). The temperature of the wall $T_w(r_i, t)$ at higher axial position (curves A in Figs. 5-8) was slightly higher than the temperature at lower axial position (curves B in Figs. 5-8) giving a little lower growth rate of frozen-layer. The theoretical predictions of the phase change front shown in Figs. 5 and 6 lie slightly below the experimental data.

Both Figs. 7 and 8 show that there were slightly larger differences than the previous cases (Figs. 5 and 6) between

the two wall temperatures measured at A and B. Also, the phase-change front velocity at the lower axial position B, where the tube wall temperature is lower, is substantially larger than at A. The agreement between the theoretical curves of the frozen-layer thickness versus time obtained from the present optimization technique and experimental data is fairly good and consistent.

5. CONCLUDING REMARKS

Experiments on the solidification of an initially stagnant superheated liquid on the outside wall of a convectively cooled vertical tube were carried out to obtain the experimental data of (1) the phase change front position versus time and (2) the transient temperature of the tube wall on which solidification is taking place. A comparison of the experimental data with the predictions of the optimization technique(Choi, et al, 1985), has indicated that the transient phase change front can be predicted by measuring the temperature of the surface on which freezing occurs. The optimization technique has a great potential in the predictions of the phase change front. This method is suitable, in particular, to obtain the knowledge of the transient phase change interface where direct measurements or photographic recordings are not possible, whereas the measurement of the convectively cooled surface temperature is relatively easy.

REFERENCES

- Carslaw, H.S. and Jaeger, J.C., 1959, "Conduction of Heat in Solids", Oxford University Press, New York, 2nd Ed, Chap. 11, pp. 283~296.
- Choi, H.O. and Chun, M.H., 1985, "Prediction of the Phase Change Front Using the Optimization Technique", Int. Comm. Heat Mass Transfer, Vol. 12, pp. 647~656.
- Chun, M.H., Gasser, R.D., Kazimi, M.S., Ginsberg, T. and Jones, O.C. Jr., 1976, "Dynamics of Solidification of Flowing Fluids with Applications to LMFBR Post-Accident Fuel Relocation", Proc. of the Int. Mtg. on Fast Reactor Safety and Related Physics, Vol. IV, pp. 1808~1818.
- Chun, M.H., and Chung, S.W., 1985, "Analysis of Forced Convection Melting in a Vertical Channel for Applications to LMFBR Post-Accident Fuel Relocation", Proc. of Third Int. Topical Mtg. on Reactor Thermal Hydraulics, pp. 19. D-1-19. D-7.
- Epstein, M., Stachyra, L.J. and Lambert, G.A., 1980, "Transient Solidification in Flow into a Rod Bundle", J. Heat Transfer, Vol. 102, pp. 330~334.
- Gupta, R.S. and Kumar, A., 1985, "Treatment of Multi-Dimensional Moving Boundary Problems by Coordinate Transformation", Int. J. Heat Mass Transfer, Vol. 28, pp. 1355~1366.
- Hale, D.V., Hoover, M.J. and O'Neill, M.J., 1971, Phase Change Material Handbook, NASA CR-61363.
- Ho, C.J. and Viskanta, R., 1984, "Inward Solid-Liquid Phase-Change Heat Transfer in a Rectangular Cavity with Conducting Vertical Walls", Int. J. Heat Mass Transfer, Vol. 27, pp. 1055~1065.
- Luenberger, D.G., 1973, "Introduction to Linear and Non-linear Programming", Addison-Wesley, Massachusetts, Chap. pp. 134.
- Shamsundar, N. and Srinivansan, R., 1979, "A New Similarity Method for Analysis of Multi-Dimensional

Solidification", J. Heat Transfer, Vol. 101, pp. 585~591.

Siegel, R., 1982, "Analysis of Solidification Interface Shape Resulting from Applied Sinusoidal Heating", J. Heat Transfer, Vol. 104, pp. 13~18.

Sparrow, E.M., Pantankar, S.V. and Ramadhyani, S., 1977, "Analysis of Melting in the Presence of Natural Convection in the Melt Region", J. Heat Transfer, Vol. 99, pp. 520~526.

Sparrow, E.M., Ransley, J.W., and Kemink, R.G., 1979,

"Freezing Controlled by Natural Convection", J. Heat Transfer, Vol. 101, pp. 578~584.

Sparrow, E.M., and Hsu, C.F., 1981, "Analysis of Two-Dimensional Freezing on the Outside of a Coolant-Carrying Tube", Int. J. Heat Mass Transfer, Vol. 24, pp. 1345~1357.

Stefan, J., 1981, "Über die Theorie der Eisbildung, insbesondere Über die Eisbildung in Polarmeere", Ann. Phys. Chem., Vol. 42, pp. 269.

KSME/JSME Vibration Conference'87

August 25-27, 1987

Korea Advanced Institute of Science and Technology
Seoul, Korea

sponsored by :

Korean Society of Mechanical Engineers
Japan Society of Mechanical Engineers

You are invited to participate in KSME/JSME Vibration Conference '87, which will be held from August 25 to 27, 1987 at KAIST, Seoul, Korea.

The conference program will include five invited lectures and over eighty contributed papers from Korea, Japan, China, and Malaysia in the subjects of Machine Dynamics, Vehicle Dynamics, Modal Analysis, Dynamic Reanalysis, Signal Processing, Simulation and Modelling/Identification, Vibration Monitoring and Control, Instrumentation; Sensors and Actuators, Time Series and Discrete Control, Diagnostics/Signature Analysis, Vibration Isolation, and other applications in vibration. During the conference, vibration-related products and services, including modal testing and analysis, will be exhibited so that users and vendors can exchange ideas about future directions in vibration research. Along with the exhibitions of instruments, demonstrations of vibration-related computer software are also scheduled.

For further details, please contact :

Professor Jang Moo Lee
Vice Chairman of the Conference Executive Committee
Department of Mechanical Design and Production Engineering
Seoul National University
Kwanak-Ku, Seoul 151, Korea
Tel.: (02)886-0101(Ext.3484)